

Multiple flares caused by mass ejection episodes during the advanced nebular phase of Nova Scuti 2019

U. Munari,^{1*} G. L. Righetti,² and S. Dallaporta,²

¹*INAF Astronomical Observatory of Padova, 36012 Asiago (VI), Italy*

²*ANS Collaboration, c/o Astronomical Observatory, 36012 Asiago (VI), Italy*

Accepted XXX. Received YYY; in original form ZZZ

ABSTRACT

Our photometric and spectroscopic monitoring shows that starting with 2020 June 4, day +217 from optical maximum and well into its advanced nebular stage, Nova Sct 2019 begun displaying a series of nine large amplitude flares (up to $\Delta m \sim 1.7$ mag), characterized by a rapid rise to peak (≤ 10 hours) and a fast exponential decline (e -folding time ~ 50 hours). The time interval Δt between flares follows an ordered sequence, declining from 8.43 to 4.90 days, that safely allows to exclude that any other flare occurred without being recorded by the observations. When the sequence of flares was over by 2020 July 28 (day +271), Nova Sct 2019 slowed its overall decline rate from $\Delta m = 0.0067$ mag/day to 0.0027 mag/day. The flares were caused by material expelled at high velocity (~ 1000 km/s) from the still burning WD. The cooler pseudo-photosphere forming at each flare in the expelled material, resulted in a recombination wave to spread through the original nova ejecta (at ~ 170 AU from the WD), quenching emission from [FeX] and [FeVII] and boosting that from lower ionization species. After each flare, once the small amount of expelled material had turned optically thin, the original nova ejecta resumed displaying [FeX] and [FeVII] emission lines, a fact that clearly proves the direct photo-ionization action exerted on the ejecta by the burning WD. While the other known flaring novae (V458 Vul, V4745 Sgr, and V5588 Sgr) presented the flares close to maximum brightness and with increasing Δt , Nova Sct 2019 is unique in having displayed them during the advanced nebular stage and with decreasing Δt .

Key words: stars: novae, cataclysmic variables

1 INTRODUCTION

The details of the multiple discoveries and designations of Nova Scuti 2019 (NSct19 for short) were given by Green (2019). The transient was first discovered by K. Nishiyama (Japan) on Oct 29.397 UT (HJD 2458785.897) at unfiltered 9.4 magnitude, resulting in transient designation TCP J18395972-1025415 when reported to CBAT, and independent discoveries by H. Nishimura and S. Kaneko (also from Japan) were soon reported to CBAT by S. Nakano. On Oct 29.524 UT, via VSNET-alert 23669, P. Schmeer noted the coincidence of TCP J18395972-1025415 with the new and unclassified transient ASASSN-19aad discovered by the ASASSN survey on Oct 29.05 (HJD 2458785.55) at $g = 11.5$ mag. Schmeer also noted the positional coincidence with a feeble progenitor source recorded by PanSTARR-S1 at $i = 20.8$ and $z = 20.0$ mag (and undetected in g and r),

and based on the apparent great outburst amplitude, he suggested the object likely to be a nova. Confirmation as a nova came soon afterward by Williams et al. (2019) via spectroscopic observations obtained on Oct 29.81 UT with the Liverpool telescope, which revealed several broad emission lines flanked by P-Cyg absorptions, features that were also noted by Pavana, Anupama, & Kumar (2019) on their spectroscopic observations for Oct 29.54 UT. A description of the early evolution of profiles of emission lines and associated P-Cyg absorptions was provided by Jack et al. (2020), who recorded a series of six high resolution spectra covering the first \sim two weeks of the outburst. The TNS server assigned the designation AT2019tpb to the transient and the General Catalog of Variable Stars (GCVS) provided the permanent designation V659 Sct.

Not much else was reported about NSct19 during the rest of 2019, with the exception of a pointing with the X-ray/UV *Swift* satellite by Sokolovsky et al. (2019), that did not detect the nova in the X-rays and recorded it at

* E-mail: ulisse.munari@inaf.it

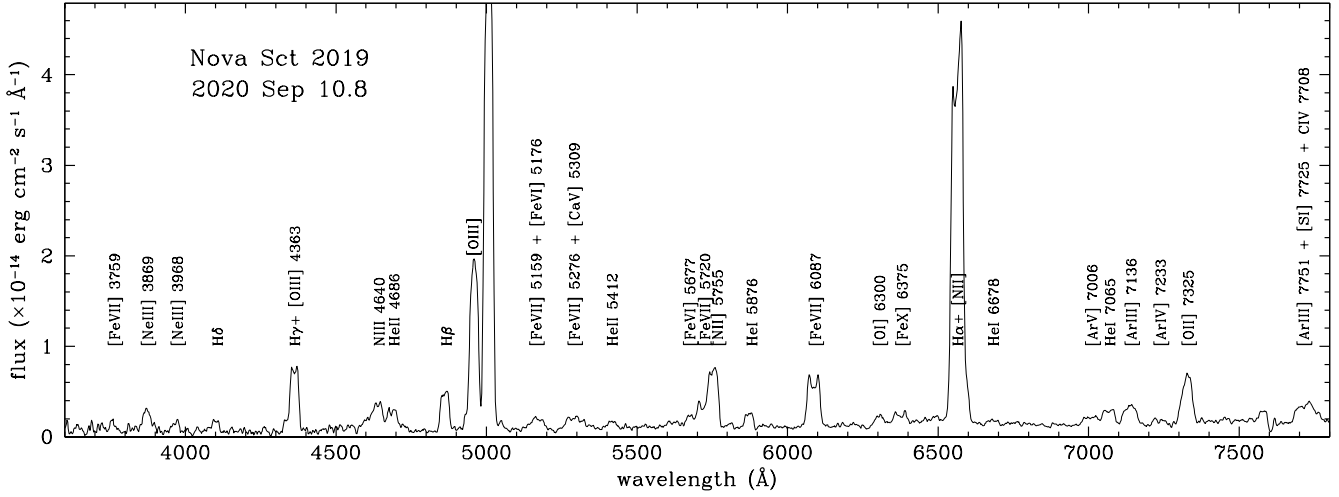


Figure 1. Spectrum for 10 Sept 2020 (day +316 from outburst maximum), representative of all the others we have recorded during our 2020 observing campaign of Nova Sct 2019, while it was going through its advanced nebular decline. The strongest lines are identified.

Table 1. Our BVRI photometry on the Landolt system of Nova Sct 2019. The complete table is only available in electronic as supplementary material; a portion is shown here to provide guidance on its content. HJD is the heliocentric JD–2450000.

HJD	B	err	V	err	R	err	I	err	ID
9023.483	15.799	0.024	14.778	0.023	14.038	0.014	13.887	0.015	1507
9023.491	15.769	0.012	14.729	0.013	14.033	0.010	13.801	0.012	0310
9024.408	15.884	0.017	14.908	0.015	14.285	0.012	14.133	0.024	1507
9024.496	15.924	0.014	14.931	0.013	14.279	0.010	14.173	0.012	0310

Table 2. Log spectroscopic observations recorded with Asiago 1.22m + B&C + 300 ln/mm (3300-8000 Å, 2.3 Å pix⁻¹).

date	UT middle	expt (sec)	HJD (-2450000)
2020 Jun 28	22:34	3600	9029.440
2020 Jul 05	00:03	4800	9035.502
2020 Jul 06	00:02	5400	9036.502
2020 Aug 20	21:37	1080	9082.401
2020 Aug 25	20:49	1080	9087.367
2020 Aug 27	19:39	1140	9089.319
2020 Sep 09	19:48	1200	9102.325
2020 Sep 10	20:03	1800	9103.335
2020 Sep 11	19:52	1200	9104.328

UVM2=14.27 mag in the ultraviolet, which led them to estimate the reddening as $E_{B-V} \sim 0.9$.

The interest in NSct19 was briefly renewed the following year by Woodward, Banerjee, & Evans (2020) that reported detecting [SiVI], [SiVII], [CaVII] and [FeIX] coronal emission lines in an infrared spectrum of the nova they recorded on 2020 June 6 with IRTF. This triggered our interest in the nova and by the following day, 2020 June 19, we began a BVRI photometric and 3300-8000 Å spectroscopic monitoring that covered the rest of the observing season for the nova up to its Solar conjunction in late October 2020. Shore & Sims (2020) obtain a low-resolution optical spectrum of NSct19 on 2020 June 19, revealing the nova to be well into its nebular stage, and confirmed the high excitation conditions seen by Woodward, Banerjee, & Evans (2020) in the infrared by detecting the coronal [FeX] 6375 Å in emission among a rich assortment of double-peaked emission lines distributed over a wide range of ionization conditions (from [OI] to [FeVII]).

In this paper we discuss the results of our monitoring of NSct19 during 2020, which coincide with its advanced nebular decline, focussing in particular on the surprising appearance of a series of very fast (~ 2 days duration) and large amplitude flares (up to $\Delta B = 1.7$ mag).

2 OBSERVATIONS

We have obtained BVRI optical photometry of NSct19 in the Landolt (2009) photometric system from 2020 June 19 to September 18 at \sim daily cadence, and then three more every \sim ten days to October 16, with ANS Collaboration telescopes ID 0310 and 1507; when close in time their data were not combined, to provide a mutual check. Data reduction has involved all the usual steps for bias, dark and flat with calibration images collected during the same observing nights. We adopted aperture photometry because the sparse field around NSct19 did not required a PSF-fitting approach. The transformation from the local to the Landolt standard system was carried out via nightly colour equations calibrated on a photometric sequence recorded on the same frames with NSct19 and extracted from the APASS DR8 survey (Henden & Munari 2014), ported to the Landolt (2009) system via the transformations calibrated by Munari et al. (2014a). Our photometry of NSct19 is listed in Table 1. The quoted errors are the quadratic sum of the Poissonian error on the variable and the error in the transformation to the standard system via colour equations.

Low resolution spectroscopy of NSct19 has been ob-

Table 3. Summary of basic parameters for Nova Sct 2019.

names	Nova Sct 2019 V659 Sct TCP J18395972-1025415 ASASSN 19aad AT 2019tpb
equatorial	RA = 18:39:59.82 DEC = -10:25:41.9
Galactic	$l = 022.352$ $b = -02.227$
outburst: maximum	UT = 2019 Oct 31.0 $V = 8.38$ mag type = FeII
decline	$t_2 = 7.0$ days $t_3 = 13.5$
amplitude	$\Delta I \sim 14.4$ mag
reddening	$E_{B-V} = 1.1$
distance (from t_3)	5.3 kpc

Table 4. Average values for the interstellar KI line we measured on Jack et al. (2020) spectra of Nova Sct 2019.

RV_{\odot} (km/s)	FWHM (km/s)	equiv. width (Å)	E_{B-V} (mag)
-8.3 ± 0.2	19	0.206 ± 0.003	0.81
$+33.3 \pm 1.2$	29	0.080 ± 0.004	0.30

tained with the 1.22m telescope + B&C spectrograph operated in Asiago by the Department of Physics and Astronomy of the University of Padova. The CCD camera is a ANDOR iDus DU440A with a back-illuminated E2V 42-10 sensor, 2048×512 array of 13.5 μm pixels. A 300 ln/mm grating blazed at 5000 Å results in 2.3 Å pix^{-1} dispersion and 3300-8000 Å spectral coverage. The slit has always been rotated to the parallactic angle for optimal flux mapping. All data have been similarly reduced within IRAF, carefully involving all steps connected with correction for bias, dark and flat, sky subtraction, wavelength calibration and heliocentric correction. The spectra have been flux calibrated against observations of the nearby spectrophotometric standard HR 7032 (2° angular distance) observed each night immediately before or after NSct19, and the zero-points checked against the result of simultaneous ANS Collaboration *BVRI* photometry. A log of the spectroscopic observations is given in Table 2.

3 BASIC PARAMETERS OF NOVA SCT 2019

Observing conditions at the time of discovery were far from ideal, with the object low on the horizon for the fast approaching Solar conjunction, and the Moon at short angular distance. Interpolating the AAVSO lightcurve with a spline function, the time of maximum in *V*-band is derived as Oct 31.0 (± 0.5) UT at $V=8.38(\pm 0.1)$, with *B* band anticipating by \sim half a day and *R*, *I* bands delayed by \sim half a day

Table 5. FWHM (corrected for instrumental resolution) and velocity separation of double peaks for some representative lines in the spectrum of Figure 1.

line	FWHM (km s $^{-1}$)	peaks (km s $^{-1}$)
HeI 7065	1930	1090
H α	1950	1280
HeII 4686	2200	1320
[OIII] 4363	2200	1380
[FeVII] 6987	2210	1450
[FeX] 6375	2450	1550
[OI] 6300	1430	
[OII] 7325	1480	
[OIII] 5007	1930	
[NeIII] 3869	2550	

from *V*-band, as expected from an expanding fireball (eg. Munari, Hambusch, & Frigo 2017). A spectrum taken shortly after maximum brightness is available in the ARAS database (Teyssier 2019), and it shows NSct19 belonging to the FeII-class of novae (Williams 1992). ASASSN observed the field of NSct19 for only a couple of days into the outburst because of the approaching Solar conjunction, deriving $g \geq 17.0$, $g=11.57$, and $g=9.54$ for Oct 28.06, Oct 29.06, and Oct 30.06 UT, respectively.

van den Bergh & Younger (1987) list +0.23 and -0.02 as the intrinsic $(B-V)_{\odot}$ colour for novae at maximum and t_2^V , respectively. From a spline interpolation of the AAVSO lightcurve we estimate $B-V \sim 1.56(\pm 0.15)$ at maximum and $B-V \sim 1.1(\pm 0.10)$ at t_2^V , corresponding to $E_{B-V}=1.3$ and 1.1 mag, respectively. VSNET CCD photometry for Oct 30.07 UT (observer K. Yoshimoto) provides $V=8.59$ and $B-V=1.20$, resulting in $E_{B-V}=1.0$ mag. Jack et al. (2020) reported about saturated multi-components for the interstellar NaI lines recorded on their TIGRE high resolution spectra. On our request, D. Jack kindly forwarded us such spectra, and on them we measured the unsaturated, multi-component profile of the KI 7699 Å interstellar line, obtaining the values listed in Table 4. By adopting the calibration of Munari & Zwitter (1997), the equivalent width of the two KI components translate into a total reddening $E_{B-V}=0.81 + 0.30 = 1.11$ mag. On the same TIGRE spectra, we also measured an average 0.2568 Å equivalent width for the diffuse interstellar band (DIB) at 6614 Å. Adopting for such DIB the calibration by Munari (2014), its equivalent width translates to $E_{B-V}=1.13$ mag. Averaging over the various estimates, we derive $E_{B-V}=1.10 (\pm 0.05)$ as the reddening affecting NSct19.

Selvelli & Gilmozzi (2019) have re-calibrated the standard MMRD relation (mag at maximum vs. rate of decline) on GAIA DR2 parallaxes. Applying it to the above $t_3^V=13.5(\pm 0.7)$ days leads to an absolute magnitude $M(V)=-8.7$ and, by combining with $E_{B-V}=1.10$ for a standard $R_V=3.1$ reddening law (Fitzpatrick 1999), to a distance of 5.3 kpc to NSct19. At such a distance, the Bayestar2019 3D model of Galactic extinction by Green et al. (2019) returns $E_{g-r} \geq 0.96$.

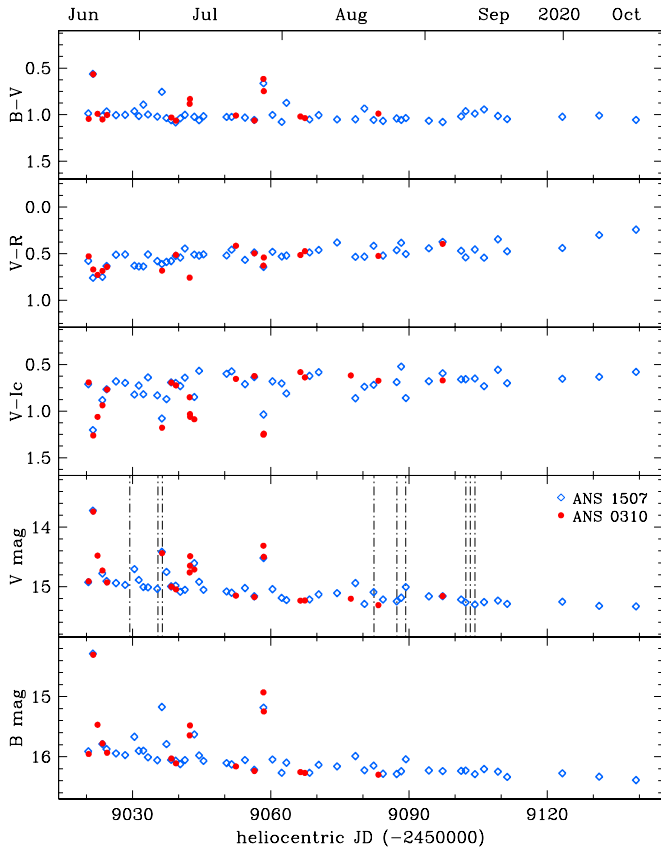


Figure 2. Photometric evolution of Nova Sct 2019 during the advanced nebular phase from our *BVRI* photometric observations in June–October 2020 (Table 1). The vertical lines in the *V*-band panel mark the epochs of our spectra listed in Table 2.

Table 3 summarizes the basic parameters of NSct19.

4 BRIGHT FLARES DURING THE ADVANCED NEBULAR PHASE

When we began our monitoring of NSct19 in June 2020, the nova was already well into its advanced nebular stage as illustrated by the spectrum in Figure 1, where [OIII] 4959, 5007 stand out prominently and stronger than H α . Considering the large intensity of [NII] 5755, some unresolved emission from [NII] 6548, 6584 probably contribute to the H α profile. The spectrum in Figure 1 is well representative of our entire June–October observing period, and well supports the reports by Woodward, Banerjee, & Evans (2020) and Shore & Sims (2020) for the presence of coronal emission lines in the infrared and optical spectra of the nova they recorded in June 2020. [FeX] 6375 is clearly present in our spectra (for a recent census of novae showing [FeX] see Rudy et al. (2021)), as well as a full assortment of [FeVI] and [FeVII] lines in addition to [ArIII], [ArIV] and [ArV] transitions. Their profiles range in shape from Gaussian-like to double-peaked, with Table 5 listing the FWHM (corrected for instrumental resolution) and separation of peaks for some representative lines. Our FWHMs are remarkably close to those measured by Jack et al. (2020) during the first two weeks of the outburst. No emission component is visible in

our spectra to match the higher velocities characterizing the P-Cyg absorptions tracked by Jack et al. (2020).

The photometric evolution of NSct19 as recorded by our June–October 2020 observations is presented in Figure 2. It is characterized by a rather slow decline in brightness ($\Delta V=0.5$ mag in 120 days), as typical of novae during the advanced nebular stage.

The most striking feature of the NSct19 lightcurve in Figure 2 is however the presence of a number of *flares*, short-lived brightenings of between 0.4 and 1.7 magnitudes in *V* and *B*, which are superimposed onto the otherwise normal and smooth decline. Such events are extremely rare in novae (see discussion below in sect. 6.2) and flag NSct19 with special interest. These flares should not be confused with the jitters many slow novae present much earlier in their evolution, during the long plateau they experience around maximum brightness (eg. Strope, Schaefer, & Henden 2010), or around the transition from optically thick to thin conditions (eg. Payne-Gaposchkin 1964).

To put the detection of flares into context, in Figure 3 we have built a more comprehensive lightcurve of NSct19 for 2020, by combining our *B*-band data with *g*-band measurements collected by ASASSN (Shappee et al. 2014; Kochanek et al. 2017) and ZTF patrol surveys (Masci et al. 2019; Bellm et al. 2019), that we have retrieved from their respective databases. An offset has been applied to *g*-band data (+0.7 mag for ASASSN, +0.9 mag for ZTF) to bring them on the same scale of *B*-band data.

The photometric decline of NSct19 during 2020 has been characterized by two different slopes, as clearly visible in Figure 3: an initial (February through July) faster decline at 0.0067 mag day $^{-1}$, followed by a slower one at 0.0027 mag day $^{-1}$. The flares appeared at the end of the faster-decline portion of the lightcurve, and they ceased as NSct19 settled onto the slower-decline descent. The change in the decline speed has been probably governed by some adjustment in the recombination vs photo-ionization of the ejecta, which may have been driven by changes in rate of nuclear burning on the central WD and/or changes of its outflowing wind, and by the possible injection of new material in the inner circumstellar space as a result of the repeated flares.

The lower panel of Figure 3 zooms on the time interval covered by the flares, which are highlighted by the yellow vertical bands. They are 9 in number and their epochs are listed in Table 6. The flares seem to follow a precise temporal sequence, as illustrated by Figure 4 where we have plotted the time interval between two successive flares. A tight linear trend is obvious, and the small deviations from it could be easily accounted for by the limited accuracy to which the time of maxima can be derived with the available data (sampling time ~ 0.5 day). Extrapolating the linear trend outside the recorded 9 flares allow to predict the times of occurrence for any further such event preceding or following those actually observed, and such times are marked with pink arrows in the lower panel of Figure 3. The arrows coincide in time with observations that caught NSct19 at the normal quiescence level, excluding that any further flare has occurred without being recorded by observations (at least any other flare obeying to the linear trend of Figure 4).

If the *e*-folding time for the brightness decline appears to be similar for all flares, approximately 50 hours, their am-

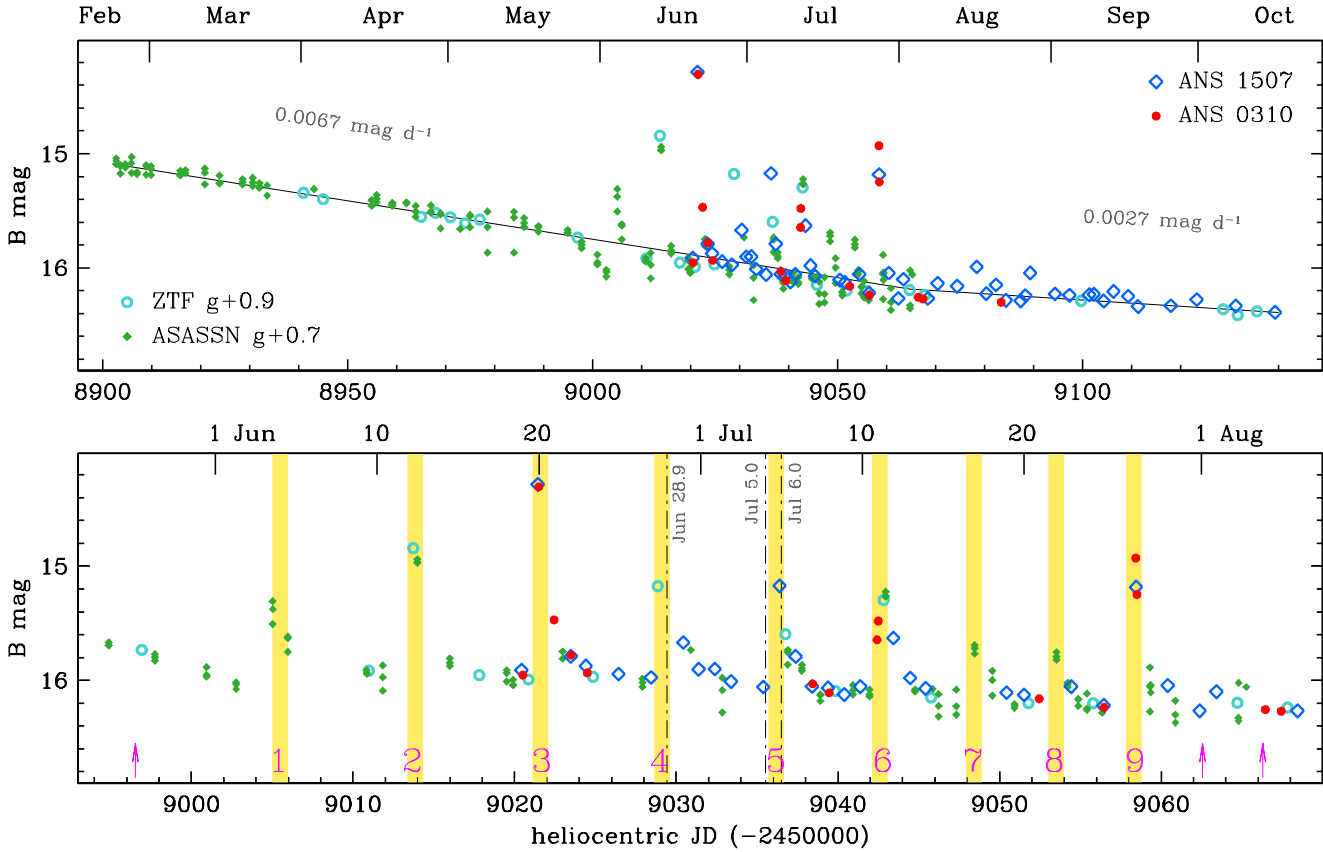


Figure 3. *Top panel:* B -band lightcurve of Nova Sct 2019 covering 2020, built from our data in Table 1 and g -band data from ASASSN and ZTF sky-patrol surveys, scaled by the indicated quantities to match the B -band data. *Bottom panel:* zooming onto the June-July portion of the lightcurve from the above panel to highlight the 9 flares experienced by the nova. The dot-dashed vertical lines mark the epoch of the three spectra discussed in Figure 6. For the meaning of the three pink arrows see text (sect. 4).

Table 6. Epochs of the nine flares exhibited by Nova Sct 2019. They correspond to the brightest photometric observation recorded for the given event, by either us, ASASSN, or ZTF. Given the sparse sampling, the actual epoch of true peak brightness may differ up to ~ 0.5 day from the listed values.

flare N.	HJD (-2450000)	UT date (2020)
1	9005.302	June 4.802
2	9013.731	June 13.231
3	9021.440	June 20.940
4	9028.855	June 28.355
5	9036.398	July 05.898
6	9042.828	July 12.328
7	9048.455	July 17.955
8	9053.527	July 23.027
9	9058.422	July 27.922

plitude may have not been always the same, with flare N.3 peaking at $\Delta B=1.7$ and N.7 and 8 limited to $\Delta B=0.4$ mag. Any definitive conclusion about flare amplitude is hampered by the sampling time of the observations (~ 0.5 days) and the real possibility that the true maximum has been missed altogether for some of them.

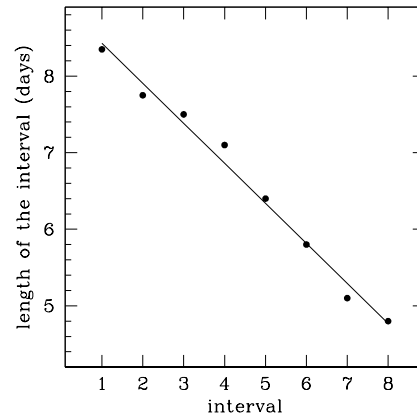


Figure 4. Length (in days) of the eight intervals between the successive nine flares listed in Table 6.

The takeaways from this section are: (1) a series of 9 fast-evolving and large-amplitude flares have been recorded during the advance nebular decline, just prior to a major change in the rate of decline of NSct19; (2) the flares are arranged in a time sequence that allows safely to conclude that all events have been recorded and none has gone unnoticed; and (3) not all flares attained the same brightness amplitude.

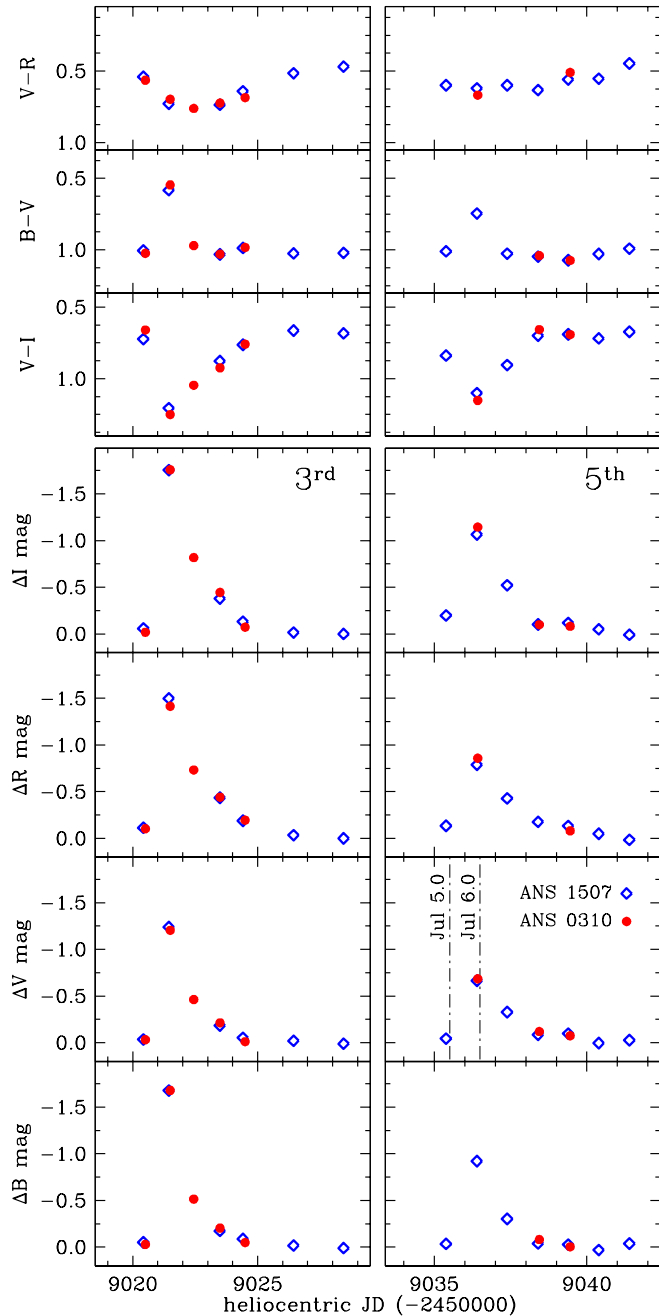


Figure 5. Expanded view of the lightcurve in Figure 2 to highlight the evolution of Nova Sct 2019 during the 3rd and 5th flares, those best covered by our *BVRI* observations.

5 ANATOMY OF THE FLARES

The observations we collected allow to document in detail the photometric and spectroscopic characteristics of the flares experienced by NSct19. The flares best covered by our photometry are the 3rd and the 5th, and Figure 5 provides a zoom on their *BVRI* light- and colour-curves: the two flares behaved very similarly and the apparent difference in peak brightness is probably an effect of the sampling by the observations.

5.1 Photometric properties

The rise to maximum brightness for all flares has been very fast. Our sampling time interval put a general $\lesssim 1$ -day upper limit to that. A more stringent value can be derived from the evolution of flare N.4 (cf. Figure 3). When we observed NSct19 on June 27.940 UT it was still at the normal quiescent level observed between flares, but shortly afterward, on June 28.355 UT, ZTF caught the nova one magnitude brighter and close to peak flare brightness, implying an upper limit to the rise to maximum brightness of ≤ 10 hours.

The photometric colour-change associated to the flares is rather peculiar, as illustrated by Figure 5: at peak of the flare, NSct19 becomes *bluer* in *B–V* by 0.5 mag, and *redder* by 0.5 mag in *V–I*, while *V–R* remains rather flat. In other words, the amount of brightening is larger at both ends of the optical range (*B* and *I* bands) than it is in the middle (*V* and *R* bands).

Both the continuum and the emission lines contribute to the flux recorded through the photometric bands, and disentangling the respective roles played during flares is impossible on purely photometric grounds. Accurately fluxed spectra are required to this aim. Luckily, two of our spectra (June 28.94 and July 06.00 UT, cf. Table 2) were obtained close in time to the peak of the 4th and 5th flares, while a third (Jul 05.00 UT) was observed during the brief quiescence in between them (their epochs are marked by the dot-dashed vertical lines in Figure 3). These three spectra are compared in Figure 6. The spectra at flare maxima look almost identical, as are the colour- and light-curves for the 3rd and 5th flares presented in Figure 5. Such similarities support the notion that the mechanism driving the flares has been one and the same throughout the whole series of nine recorded events.

Given their similarities, we have averaged the two spectra at flare maximum and subtracted from them the spectrum for the in-between quiescence. The resulting difference-spectrum is plotted in the lower panel of Figure 6. We have then integrated the flux of the spectra in Figure 6 through the transmission profile of the *BVRI* photometric bands as tabulated by Landolt (1992), with the zero-points being fixed by repeating an identical operation on the spectrophotometric standards observed along with NSct19. The resulting magnitudes are listed in Table 7, where we also report the photometric magnitude corresponding to the flux radiated separately in the continuum (fitted with a bremsstrahlung distribution) and in the emission lines. From Table 7 it is evident how the variation going from quiescence to flare peak is larger for the continuum (1.0 mag) than it is for the emission lines (0.4 mag). A large change affects the *4640-blend*, probably composed of NIII lines pumped by fluorescence from HeII Ly α via OIII 374.432 Å (Bowen 1947; Selvelli, Danziger, & Bonifacio 2007). The $3\times$ increase in the intensity of the 4640 blend, which is located close to the peak of the *B*-band transmission profile, seems the prime responsible for the larger amplitude (0.8 mag) in *B* compared to *V* and *R* (both 0.4 mag) for the variation due to the emission lines.

As well illustrated by Figure 6 and Table 7, in going from quiescence to flare-peak the underlying continuum brightens similarly at all (optical) wavelengths, so its shape remained unchanged. If the fluorescence-pumped NIII 4640

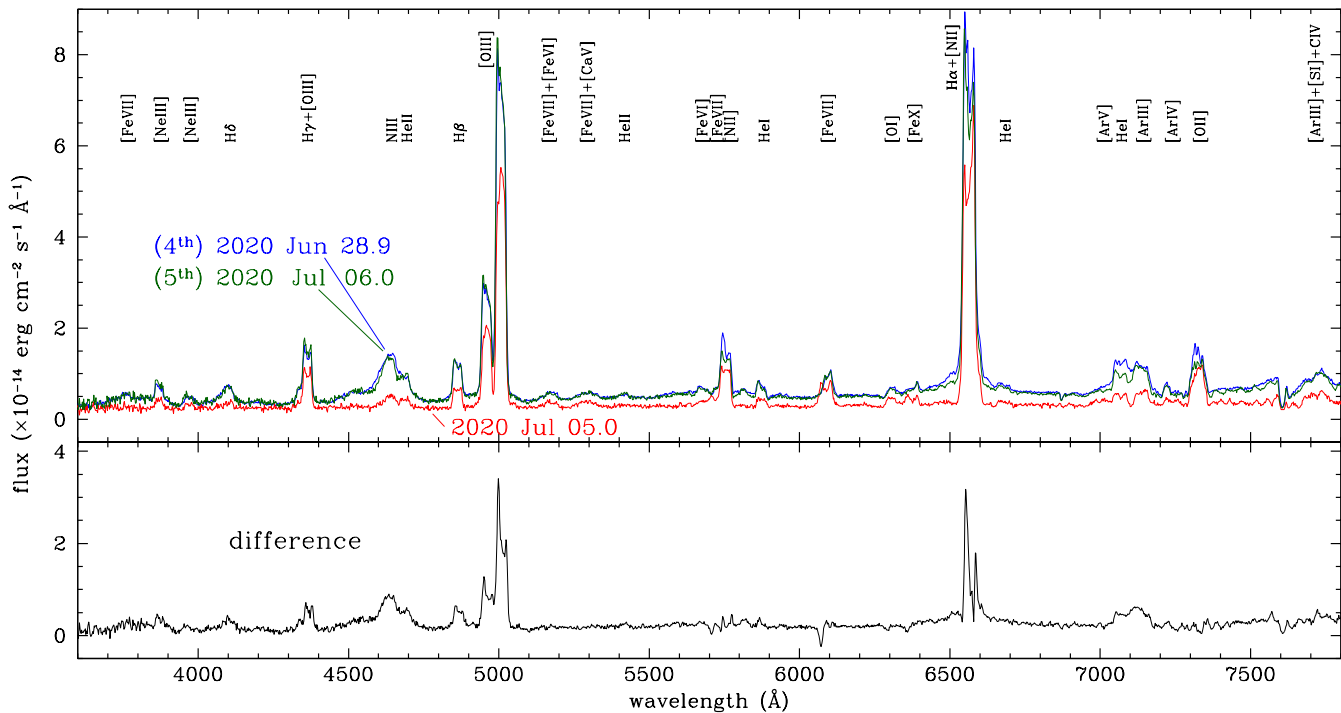


Figure 6. *Upper panel:* our spectra obtained at peak of flares N. 4 and 5 (June 28.9 and July 6.0 UT), and during the in-between quiescence (July 5.0 UT). *Lower panel:* result of subtracting the quiescence spectrum from the average of the two flare spectra.

complex may contribute to a larger brightening of NSct19 in *B* band compared to *V* and *R*, a similar role could be played for the *I* band by OI 8446 line, fluorescence-pumped by HI Ly β (Bowen 1947), and located close to the peak of the *I* band transmission profile. The OI 8446 line is rather strong in novae, frequently second only to H α in terms of emitted flux (eg. Munari et al. 2014b). Unfortunately, we cannot test this hypothesis with our spectra that do not extend redward of 8000 Å.

5.2 Changes in the emission line profiles

The type of change in the profiles of emission lines of NSct19 in going from quiescence to flare peak is illustrated in Figures 7 and 8, which zooms on spectra presented in Figure 6.

For all the emission lines, with the except of [FeVII] and [FeX], the flare causes the emission profile to develop a blue-peaked component over an otherwise flat (eg. [NII] 5755, [ArIII] 7136, HeI 5876) or rounded top ([OIII] 4959 and 5007, [OII] 7325). The radial velocity of such blue peak is -650 km/s for all lines, as indicated by the vertical lines in Figure 7.

An opposite behavior characterized the highest ionization emission lines: as illustrated by Figure 7 for [FeVII] 5720,6087 and [FeX] 6375, their line profiles in quiescence are double-peaked, with the blue peak at -650 km/s that disappears during a flare.

Going from quiescence to flare peak also causes the appearance of broad wings, albeit of low intensity, to permitted lines which have no counterparts for nebular ones, as deducible from Figure 6 by comparing H α and [OIII] lines. Figure 8 zooms on the H α wings from Figure 6, fitted with a simple Gaussian of FWHM \sim 2300 km/s.

Table 7. Photometry from flux integration on spectra of Nova Sct 2019 taken at flare peak (Jun 28.9 and July 6.0) and in-between quiescence (Jul 5.0). The central column refers to the spectra zipped of their emission lines, and the right column to the spectra subtracted of their underlying continuum (approximated by fitting to a bremsstrahlung distribution).

spectrum			continuum			em. lines		
<i>B</i>	<i>V</i>	<i>R</i>	<i>B</i>	<i>V</i>	<i>R</i>	<i>B</i>	<i>V</i>	<i>R</i>
<i>flare peak</i>								
15.17	14.47	13.74	16.05	15.13	14.39	15.84	15.33	14.64
<i>quiescence</i>								
16.06	15.18	14.46	16.97	16.20	15.39	16.68	15.72	15.06
<i>difference spectrum</i>								
15.81	15.31	14.67	16.70	15.73	15.04	16.44	16.56	16.03

6 DISCUSSION

6.1 Interpreting the flares

We assume a standard, spherical arrangement for the material ejected by the nova during the main 2019 outburst, characterized by internal and external radii and with the WD at the center (cf. Figure 9). The presence of persistent [FeX] in emission, suggests that the WD was still burning at its surface at the time of the flares, being hot and bright and thus exerting its photo-ionizing action through the optically

thin ejecta and contrasting their recombination from higher ionized states.

Averaging over the FWHM of the emission lines and the velocity of P-Cyg absorptions seen at the time of maximum brightness, we may adopt 1000 km/s as the expansion velocity of the bulk of the ejecta. In the 10 months elapsed since the outburst in Oct 2019, at the time of the flares, the ejecta have expanded to a radius of 170 AU, corresponding to a travel light-time of 2.0 days to cross the diameter of the shell. In other words, an external observer will receive news from the receding side of the ejecta only 2.0 days after being informed about the approaching one.

We believe that a flare in NSct2019 was initiated by a sudden ejection (spherical or at least bi-conical along an axis approximately oriented to the line of sight) of a limited amount of material from the central WD. The FWHM=2300 km/s broad wings visible in the $H\alpha$ flare profile of Figure 8 trace the ejected material, which mass appears much smaller than that ejected during the main outburst, as the $\sim 1:10$ ratio in the $H\alpha$ flux suggests. The material is optically thick when expelled, and remain so until after the flare peak, which marks the time when the expanding pseudo-photosphere reaches its maximum radius. The expanding pseudo-photosphere formed by the optically thick material causes a drop in the surface temperature of the central photo-ionizing source, driving a recombination wave through the ejecta. The effect is more pronounced at inner radii of the ejecta where the higher electron density allows the recombination to proceed at a faster pace. Emission from [FeVII] and [FeX] is quenched down because their recombination is no more contrasted by photoionization from the central source, and a surge is observed in the emission from lower ionization lines such as Balmer, HeI, [OI], [OII], [OIII], [NII], [ArIII] etc. populated by recombination from higher ionization states.

Our spectroscopic observations during flares (Figure 6, 7, and 8) have been obtained within hours from the recorded photometric maximum. Within such a short time interval, only light from the approaching ejecta has been able to reach the observer (the light-grey *A* portion in Figure 9 where originates the blue portion of the emission line profiles), while the rest of the ejecta (the dark-grey *B* portion in Figure 9 that produces the rest of the line profiles) still appear to the observer as it was *before* the onset of the flare. In the *A* portion of the ejecta in Figure 9, not more exposed to hard radiation from the central WD, the recombination depletes the medium from the highest ionization species (like [FeVII] and [FeX]) and as a consequence the blue peak in their double-peaked profiles fades away. At the same time, the recombination from higher ionization levels in the *A* region, increases the density of lower ionization species and boost the blue peak in their double-peaked profiles.

The return to pre-flare conditions is rather quick, the e -folding time for decline in brightness after a flare peak being ≈ 50 hours (cf. Figure 5). Unfortunately, we do not have spectra of NSct2019 obtained two or three days past the maximum brightness of a flare; we may however predict that on such spectra the ratio of blue-to-red peaks in the double-peaked profile would appeared reversed with respect to Figure 7: the strongest peak would be the blue one for [FeVII] and [FeX], and the red one for the other lines.

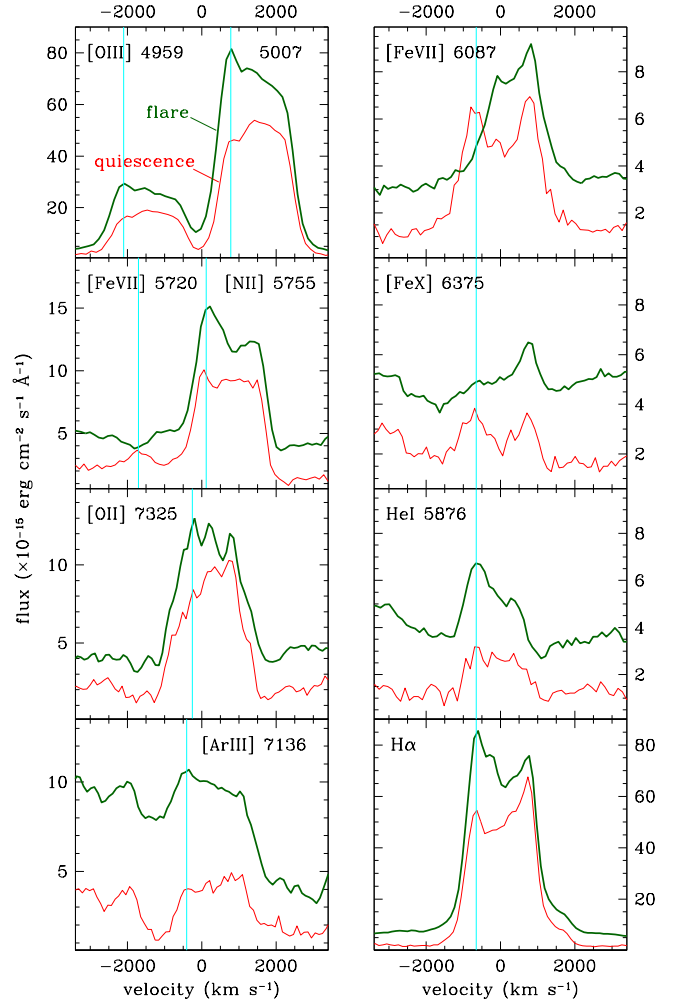


Figure 7. Comparison of the profiles of some representative emission lines in the spectra of Nova Sct 2019 in Figure 6. The profiles from the flare spectrum of July 6.0 UT are plotted in green and thicker line (higher fluxes), those for the quiescence spectrum on July 5.0 UT are in red and thinner line (lower fluxes). The vertical lines at -650 km s^{-1} mark the position of the blue peak that disappear during flares for [FeVII] and [FeX] lines and instead reinforce in all others.

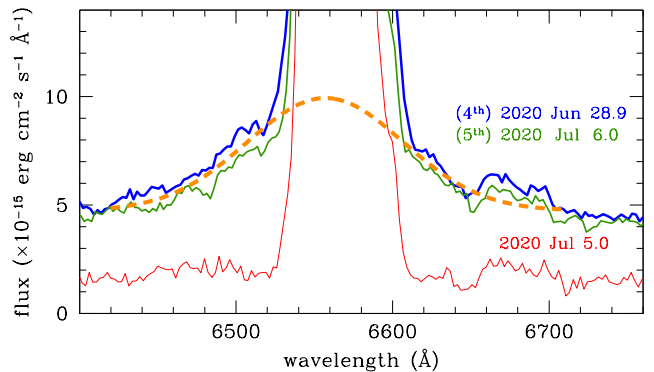


Figure 8. Zooming on the wing of $H\alpha$ for the spectra presented in Figure 6, to highlight the appearance of broad wings at flare peaks (Jun 28.9 and Jul 6.0) compared to the in-between quiescence (Jul 5.0). The dashed line is a Gaussian of FWHM=2300 km/s plotted for reference.

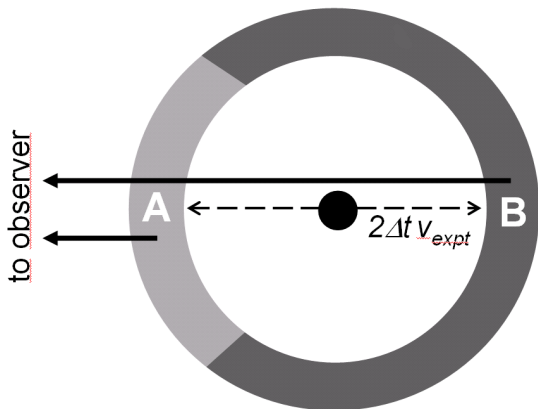


Figure 9. The simple spherical-shell geometry of the ejecta (not to scale) adopted in sect. 6.1 to explain the behavior during flares of the profiles of emission lines.

6.2 Flaring novae

Very few novae have presented sequences of quick flares in their outburst lightcurve as those displayed by NSct19.

Such events should *not* be confused with the chaotic up-and-downs that several novae present during their plateaued maxima, as shown by DQ Her, HR Del, V723 Cas, V2540 Oph, or V1405 Cas among many others (eg. Payne-Gaposchkin 1964; Kiyota, Kato, & Yamaoka 2004; Strope, Schaefer, & Henden 2010), nor with the single-secondary maxima of V2362 Cyg, V1493 Aql, or V2491 Cyg (eg. Venturini et al. 2004; Munari et al. 2008; Hachisu & Kato 2009; Arai et al. 2010; Munari et al. 2011), nor even with the (periodic) oscillation that some novae present around the time of transition from optically-thick to -thin conditions, like V603 Aql, V1494 Aql, or LZ Mus (eg. McLaughlin 1960; Warner 1995; Retter, Liller, & Garrard 2000; Retter 2003; Iijima & Esenoglu 2003). Also the rapid variability presented in quiescence by V2487 Oph (Schaefer, Pagnotta, & Zoppelt 2022) or by systems like TV Col (Scaringi et al. 2022) represent entirely different phenomena, driven by strong magnetic fields.

Our definition of a *flaring nova* is the following:

- (i) the flares appear superimposed on an otherwise smooth and normally evolving lightcurve of a nova outburst;
- (ii) the flares are isolated and very quick events, coming in sequences;
- (iii) a sequence of flares shows a clearly ordered pattern, either in terms of time-intervals and/or energy released;
- (iv) the rise-time to flare peak brightness is rather short (≤ 1 day), and the exponential decline is characterized by a quick e -folding time, of the order of a few days;
- (v) the large amplitude of the flares ($\Delta m \geq 1$ mag) makes them outstanding features of the lightcurve.

To the best of our knowledge, there are only four novae that satisfy these criteria: V458 Vul (Tarasova 2015), V4745 Sgr (Csák et al. 2005; Tanaka et al. 2011), V5588 Sgr (Munari et al. 2015), and NSct19 discussed in this paper. All of them started as FeII-type of slow/modest expansion velocities, with V458 Vul and V5588 Sgr turning hybrid (Williams

1992) at later times. All presented the [FeX] coronal emission line in their spectra, with the exception of V4745 Sgr for which the spectroscopic monitoring may have stopped too early to catch the high-ionization phase. Line profiles at the time of flares suggest that a low amount of material (much smaller than that expelled during the initial nova eruption) is ejected at high velocity.

Two main characteristics put NSct19 aside from the other flaring novae: (a) in NSct19 the flares were observed to occur at late times, during the advanced nebular phase, while for the other novae the flares appeared very early in the outburst, close to maximum brightness, and (b) the time interval between consecutive flares *decreases* in NSct19 while it *increases* for the others. There are many other differences that contributes to make the group of flaring novae rather heterogeneous, like that fact V458 Vul and V5588 Sgr did not develop a nebular spectrum contrary to V4745 Sgr and NSct19, or the photometric colours during a flare evolved in opposite directions for NSct19 and V5588 Sgr (multi-band lightcurves are not available for V458 Vul and V4745 Sgr).

A detailed comparison of the properties of the four flaring novae is well beyond the scopes of the present paper, but a comparative study would certainly be instructive to carry out (eg. Pejcha 2009), especially if supported by basic information like orbital periods and inclinations, WD mass, companion type, and presence and role of magnetic fields, all rather difficult to obtain in view of the faintness of these novae in quiescence.

7 CONCLUSIONS

The observations monitoring the evolution of novae usually rarely or even stop when they enter and progress through the nebular stage, on the wisdom that changes will be mostly slow, gradual, and predictable. Our observations of NSct19 clearly prove that this is not always the case, with the catching of rather unexpected phenomena rewarding a persisting observational effort.

NSct19 displayed flaring of a nature never before detected: between days +217 and +271 from optical maximum, nine short-lived brightenings of between 0.4 and 1.7 magnitudes in V and B were observed, all rather similar in their photometric and spectroscopic development. At the time the nova was still burning nuclearly at the surface of the WD and well into the advanced nebular stage, ~ 7 mag below maximum brightness, and with optical and IR spectra displaying forbidden lines of a high ionization degree (eg. [ArV], [FeVII], [FeX]). The flares appeared all of a sudden, without precursor events, and the sequence neatly stopped after the ninth flare. The time interval between the flares followed an ordered sequence, declining linearly from 8.43 to 4.90 days, that safely allows to exclude that any other flare occurred without being recorded by the observations. The color and spectroscopic evolution of the flares indicates that their origin resides in repeated episodes of mass ejection from the WD.

A few other novae have been noted to show flares, but they appeared very early in the outburst, close to maximum brightness, and with the time interval between consecutive flares increasing, while it was instead decreasing for NSct19. Available observations not always allow to constrain

the origin of the flares, but at least for V5588 Sgr they were traced to episodic mass ejections from the WD, similarly to NSct19.

ACKNOWLEDGEMENTS

We thank the Referee (Stewart Eyres) for valuable suggestions. We also acknowledge the support by to P. Valisa, P. Ochner, and A. Frigo to this project.

8 DATA AVAILABILITY

The data underlying this article will be shared on reasonable request to the corresponding author.

REFERENCES

- Appenzeller I., Oestreicher R., 1988, *AJ*, 95, 45. doi:10.1086/114611
- Arai A., Uemura M., Kawabata K. S., Maehara H., Nakajima K., Kiyota S., Kato T., et al., 2010, *PASJ*, 62, 1103. doi:10.1093/pasj/62.4.1103
- Bellm E. C., Kulkarni S. R., Graham M. J., Dekany R., Smith R. M., Riddle R., Masci F. J., et al., 2019, *PASP*, 131, 018002. doi:10.1088/1538-3873/aaecbe
- Bowen I. S., 1947, *PASP*, 59, 196. doi:10.1086/125951
- Csák B., Kiss L. L., Retter A., Jacob A., Kaspi S., 2005, *A&A*, 429, 599. doi:10.1051/0004-6361:20035751
- De Robertis M. M., Osterbrock D. E., 1986, *ApJ*, 301, 727. doi:10.1086/163939
- Ferland G. J., 2006, *hbic.book*
- Fitzpatrick E. L., 1999, *PASP*, 111, 63. doi:10.1086/316293
- Green, D. W. E., 2019, *CBET* 4690, 1
- Green G. M., Schlafly E., Zucker C., Speagle J. S., Finkbeiner D., 2019, *ApJ*, 887, 93. doi:10.3847/1538-4357/ab5362
- Iijima T., Esenoglu H. H., 2003, *A&A*, 404, 997. doi:10.1051/0004-6361:20030528
- Hachisu I., Kato M., 2009, *ApJL*, 694, L103. doi:10.1088/0004-637X/694/2/L103
- Henden A., Munari U., 2014, *CoSka*, 43, 518
- Jack D., Schröder K.-P., Eenens P., Wolter U., González-Pérez J. N., Schmitt J. H. M. M., Hauschildt P. H., 2020, *AN*, 341, 781. doi:10.1002/asna.202013818
- Kiyota S., Kato T., Yamaoka H., 2004, *PASJ*, 56, S193. doi:10.1093/pasj/56.sp1.S193
- Kochanek C. S., Shappee B. J., Stanek K. Z., Holoiien T. W.-S., Thompson T. A., Prieto J. L., Dong S., et al., 2017, *PASP*, 129, 104502. doi:10.1088/1538-3873/aa80d9
- Landolt A. U., 2009, *AJ*, 137, 4186. doi:10.1088/0004-6256/137/5/4186
- McLaughlin D. B., 1960, *stat.book*, 585
- Masci F. J., Laher R. R., Rusholme B., Shupe D. L., Groom S., Surace J., Jackson E., et al., 2019, *PASP*, 131, 018003. doi:10.1088/1538-3873/aae8ac
- Mendoza C., 1983, *IAUS*, 103, 143
- Munari U., 2014, *ASPC*, 490, 183
- Munari U., Zwitter T., 1997, *A&A*, 318, 269
- Munari U., Hamsch F.-J., Frigo A., 2017, *MNRAS*, 469, 4341. doi:10.1093/mnras/stx1116
- Munari U., Siviero A., Henden A., Cardarelli G., Cherini G., Dallaporta S., Dalla Via G., et al., 2008, *A&A*, 492, 145. doi:10.1051/0004-6361:200809502
- Munari U., Siviero A., Dallaporta S., Cherini G., Valisa P., Tomasella L., 2011, *NewA*, 16, 209. doi:10.1016/j.newast.2010.08.010
- Munari U., Henden A., Frigo A., Zwitter T., Bienaymé O., Bland-Hawthorn J., Boeche C., et al., 2014a, *AJ*, 148, 81. doi:10.1088/0004-6256/148/5/81
- Munari U., Ochner P., Dallaporta S., Valisa P., Graziani M., Righetti G. L., Cherini G., et al., 2014b, *MNRAS*, 440, 3402. doi:10.1093/mnras/stu547
- Munari U., Henden A., Banerjee D. P. K., Ashok N. M., Righetti G. L., Dallaporta S., Cetrulo G., 2015, *MNRAS*, 447, 1661. doi:10.1093/mnras/stu2486
- Pavana M., Anupama G. C., Kumar S. P., 2019, *ATel*, 13245
- Payne-Gaposchkin C., 1964, *gano.book*
- Pejcha O., 2009, *ApJL*, 701, L119. doi:10.1088/0004-637X/701/2/L119
- Retter A., 2003, *ASPC*, 303, 232
- Retter A., Liller W., Garrard G., 2000, *NewAR*, 44, P65
- Rudy R. J., Subasavage J. P., Mauerhan J. C., Varakian M., Rossano G. S., Puetter R. C., 2021, *AJ*, 161, 291. doi:10.3847/1538-3881/abe631
- Scaringi S., Groot P. J., Knigge C., Bird A. J., Breedt E., Buckley D. A. H., Cavecchi Y., et al., 2022, *Natur*, 604, 447. doi:10.1038/s41586-022-04495-6
- Schaefer B. E., Pagnotta A., Zoppelt S., 2022, *MNRAS*, 512, 1924. doi:10.1093/mnras/stac443
- Selvelli P., Danziger J., Bonifacio P., 2007, *A&A*, 464, 715. doi:10.1051/0004-6361:20066175
- Selvelli P., Gilmozzi R., 2019, *A&A*, 622, A186. doi:10.1051/0004-6361/201834238
- Shappee B. J., Prieto J. L., Grupe D., Kochanek C. S., Stanek K. Z., De Rosa G., Mathur S., et al., 2014, *ApJ*, 788, 48. doi:10.1088/0004-637X/788/1/48
- Shore S. N., Sims F., 2020, *ATel*, 13819
- Sokolovsky K. V., Aydi E., Chomiuk L., Kawash A., Strader J., Mukai K., Stanek K. Z., et al., 2019, *ATel*, 13252
- Strope R. J., Schaefer B. E., Henden A. A., 2010, *AJ*, 140, 34. doi:10.1088/0004-6256/140/1/34
- Tanaka J., Nogami D., Fujii M., Ayani K., Kato T., 2011, *PASJ*, 63, 159. doi:10.1093/pasj/63.1.159
- Tarasova T. N., 2015, *ARep*, 59, 920. doi:10.1134/S1063772915090085
- Teyssier F., 2019, *CoSka*, 49, 217
- van den Bergh S., Younger P. F., 1987, *A&AS*, 70, 125
- Venturini C. C., Rudy R. J., Lynch D. K., Mazuk S., Puetter R. C., 2004, *AJ*, 128, 405. doi:10.1086/421741
- Warner B., 1995, *cvs..book*
- Williams R. E., 1992, *AJ*, 104, 725. doi:10.1086/116268
- Williams S. C., Darnley M. J., Healy M. W., Murphy-Glasyer F. J., Ransome C. L., 2019, *ATel*, 13241
- Woodward C. E., Banerjee D. P. K., Evans A., 2020, *ATel*, 13815

This paper has been typeset from a \TeX / \LaTeX file prepared by the author.